Available online at www.sciencedirect.com
ScienceDirect
Coordination Chemistry Reviews 251 (2007) 2717–2731
COORDINATION CHEMISTRY REVIEWS
www.elsevier.com/locate/ccr

Review

Coordination design of artificial metalloproteins utilizing protein vacant space

Takafumi Ueno [a,c], Satoshi Abe [a], Norihiko Yokoi [a], Yoshihito Watanabe [b,*]

[a] Department of Chemistry, Graduate School of Science, Nagoya University, Nagoya 464-8602, Japan
[b] Research Center for Materials Science, Nagoya University, Nagoya 464-8602, Japan
[c] PRESTO, Japan Science and Technology Agency (JST), Japan

Received 11 January 2007; accepted 8 April 2007
Available online 12 April 2007

Contents

Abstract

Design of artificial metalloproteins is one of the most important subjects in the field of bioinorganic chemistry. In order to prepare them, vacant space of proteins has been utilized because it gives us unique chemical environment to construct catalysts and materials. This article reviews on preparation methods and properties of metal/protein composites. The discussion includes our recent results and development in the screening of composites, crystal structures, molecular design of bio-inspired systems concerning catalysts, electrochemistry, and materials.

Keywords: Myoglobin; Ferritin; Nanoparticle; Biomineralization; Metalloenzyme; Heme

1. Introduction

Coordination chemistry in protein scaffolds is an attractive target to understand various reaction mechanisms of native metalloproteins and to apply them to catalytic reactions and biotechnology [1,2]. Especially, the conjugation of metal complexes and/or materials with proteins is growing into an important topic. The design of protein-based composites will allow us to prepare metalloproteins bearing useful functions and properties. Surprisingly, Akabori et al. had already reported that Pd nanoparticles deposited on silk protein fiber catalyzed heterogeneously asymmetric hydrogenation of oximes and oxazolones [3]. More importantly, this pioneer work was done before the discovery of the first example of asymmetric catalysts using chiral transition-metal complexes reported by Noyori and co-workers [4]. Wilson and Whitesides reported the first artificial organometalloenzyme which catalyzes asymmetric olefin hydrogenation as a homogeneous catalyst [5]. However, at that

* Corresponding author. Tel.: +81 52 789 3049; fax: +81 52 789 2953.
E-mail address: taka@mbox.chem.nagoya-u.ac.jp (Y. Watanabe).

0010-8545/$ – see front matter © 2007 Elsevier B.V. All rights reserved.
doi:10.1016/j.ccr.2007.04.007

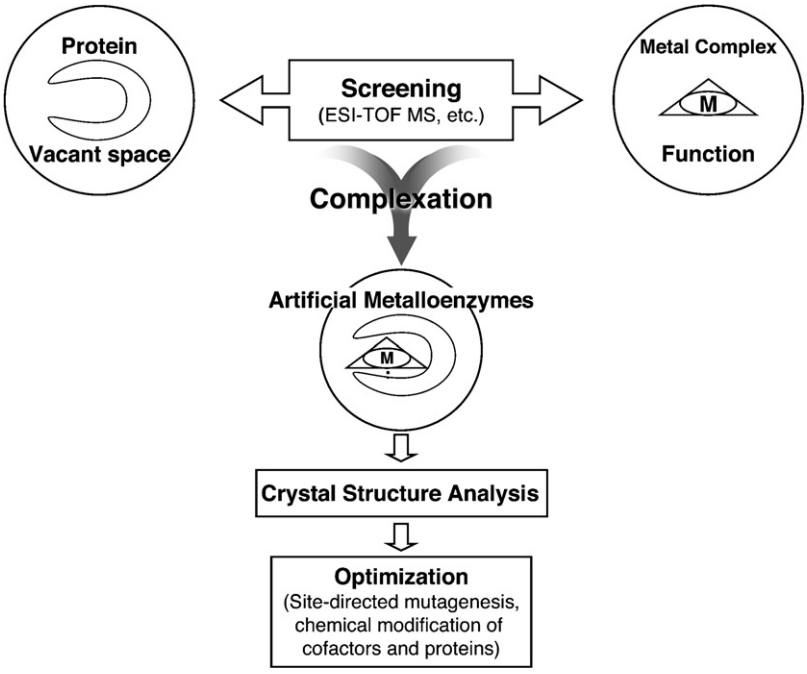

Fig. 1. Current strategy to design artificial metalloproteins utilizing protein vacant space.

time, it was too difficult to characterize and optimize its catalytic reactivity due to limitation of structural analyses and computational design of these protein composites.

Recently, rational design of metal/protein composites has attracted us because of the application of those composites to nanoscience including biotechnology, electronics, sensing, etc. by overcoming the problems mentioned above. In addition, inorganic chemists are coming to be familiar with biochemical experimental techniques such as protein mutagenesis and protein crystal structure analysis. In fact, a number of reports concerning X-ray crystal structures of metal/protein composites have greatly been increasing since 2000 [6–23]. Several researchers have also reported high-throughput screening of hybrid proteins by electrospray ionization time of flight mass (ESI-TOF MS) competition [24], computational design [25], directed evolution, etc. [26,27]. Therefore, if new strategy was developed to create useful metal/protein composites by combining the screening methods and protein crystal structure analysis as shown in Fig. 1, we will be able to obtain desired artificial metalloproteins.

The proteins and metal complexes studied since 2000 are listed in Table 1. The chemical modification of metalloproteins and hybridization of metal complexes with proteins for catalytic reactions have been main subjects as summarized in several reviews [28–32]. However, the direction of the research has been shifting to materials science aimed for biomineralization, design of metal drugs, and fine-tuning of artificial enzymes for the last several years. This suggests that the field classified as a category of bioinorganic chemistry is growing from basic science to application technology. In this review, the authors focus on the recent studies since 2002 as well as our progress.

2. Preparation of artificial metalloproteins

There are three distinct approaches for the construction of artificial metal complex/protein composites: (i) covalent insertion of unnatural metal cofactors, (ii) non-covalent insertion of unnatural metal cofactors, and (iii) accommodation of metal cations or materials in proteins. These strategies have been

Table 1
Proteins and metal complexes for the constructions of artificial metalloproteins and their functions

Protein	Metal compound	Function	References
Myoglobin	Heme derivatives	Catalyst/O_2 storage/electron transfer	[33–38]
	Cr and Mn Schiff base complexes	Catalyst	[15,24,39–41]
Avidin	Biotinated Rh and Ru complexes	Catalyst	[5,26,29,42–44]
Albumin	Heme, Cu, and Rh complexes	Catalyst/O_2 storage	[45–49]
Lysozyme	Ru and Cu complexes	Metal drug	[6,9,50–52]
Kinase	Ru complex	Inhibitor	[18,53]
Ferritin	Pd, Ag, CdS, Fe_3O_4, ZnSe clusters and Gd complex	Catalyst, material	[54–59]
Virus	Au, CoPt, and FePt clusters	Material	[60–65]
	Ferrocene derivative	Material	[66]

known very well in biosynthesis of native metalloproteins, such as cytochrome *c* (cyt *c*), myoglobin (Mb), and ferritin (Fr), respectively. For example, the heme cofactor of cyt *c* is cross-linked to the protein scaffold with covalent bonding between cys residues and vinyl groups of heme [67]. On the other hand, the heme of Mb, which functions as an oxygen carrier, is fixed in the active site by non-covalent interactions [67]. Furthermore, iron(II) cations which are introduced in Fr are oxidized and converted to $Fe^{III}{}_2O_3$ mineral [68]. Thus, we have learned how to construct the artificial composites from the biosyntheses.

2.1. Vacant spaces in various proteins for unnatural metal cofactors

It is very important to select proteins for the construction of artificial metalloproteins. In order to employ protein scaffolds as molecular templates, we should consider their stability to wide range of pH, high temperature, organic solvents and availability of crystal structures for the rational design. Proteins suitable for the accommodation of metal complexes or materials are shown in Fig. 2. Serum albumin (SA) is the most abundant protein in a circulatory system [69–71]. Its function is the transportation of hydrophobic molecules such as fatty acids, bilirubin, and steroid. The crystal structure of human SA indicates that it is capable of storing five substrates using several hydrophobic cavities at a time [13] (Fig. 2a). Thus, there are many reports attempting the use of SA to make the hybrid proteins by the conjugation of SA and several metal complexes [45–49]. Mb is known very well as a molecular scaffold that can include a metal complex or a modified heme instead of native heme in the active site (Fig. 2b) [36,37]. The affinity of heme with apo-Mb results from (i) the coordination of the proximal His93 ligand to the heme iron and (ii) hydrogen bond and hydrophobic interactions between the protein and heme [72]. Another method to introduce metal complexes into protein environment is "avidin–biotin technique" known for bio-applications (Fig. 2c) [73]. Avidin, which is composed of four identical subunits, is a very strong biotin binding protein having a large affinity constant of *ca.* $10^{15}\,M^{-1}$. Many biotin derivatives tightly fixed in the avidin-binding site have been reported [26,29,42,43,73]. Fr is known as an iron storage protein in many biological systems [68,74]. Fr is a large protein cage formed by self-assembly of 24 subunits having a molecular weight more than 440 kDa (Fig. 2d). Thousands of iron atoms can be accommodated in a hollow cage-like structure of 8 nm in diameter. The assembly is stable in a wide range of pH from 2 to 11 and at high temperature (<80 °C). It is possible to introduce many metal cations and metal complexes into the cage at once [54–58,61,74–78]. Cowpea mosaic virus (CPMV) has a particle structure showing unique characters for surface modification with metal materials [60,66,79–81]. Approximately 1 g of virus is easily and routinely obtained from a kilogram of infected leaves of the black-eye pea plant [82]. The virus con-

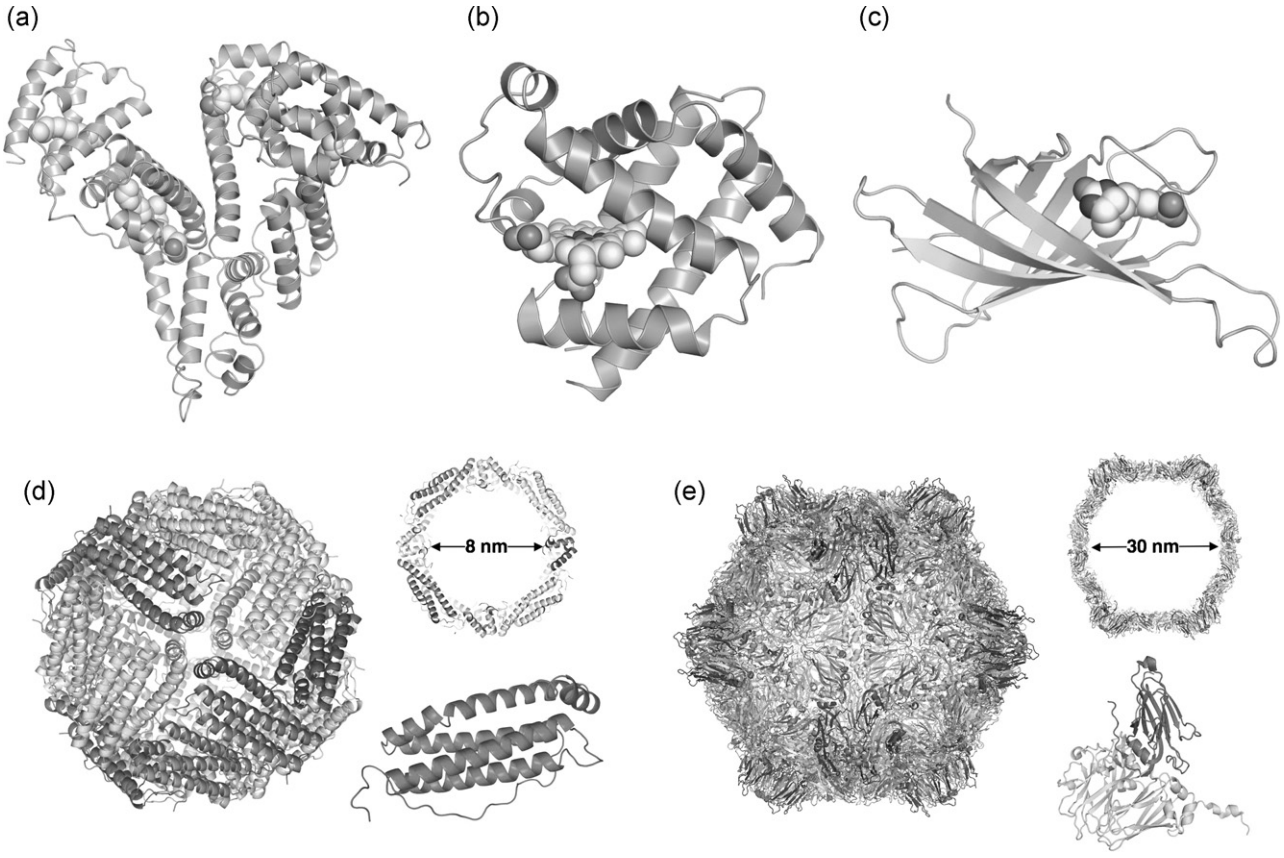

Fig. 2. Various protein scaffolds for construct of artificial metalloproteins. The crystal structures are drawn with ribbon models of (a) HSA, (b) Mb, (c) avidin, (d) Fr, and (e) CPMV. They are taken from PDB IDs of 1BJ5, 4MBN, 1AVD, 1DAT, and 1NY7, respectively. Cofactors and substrates are shown as space filling models.

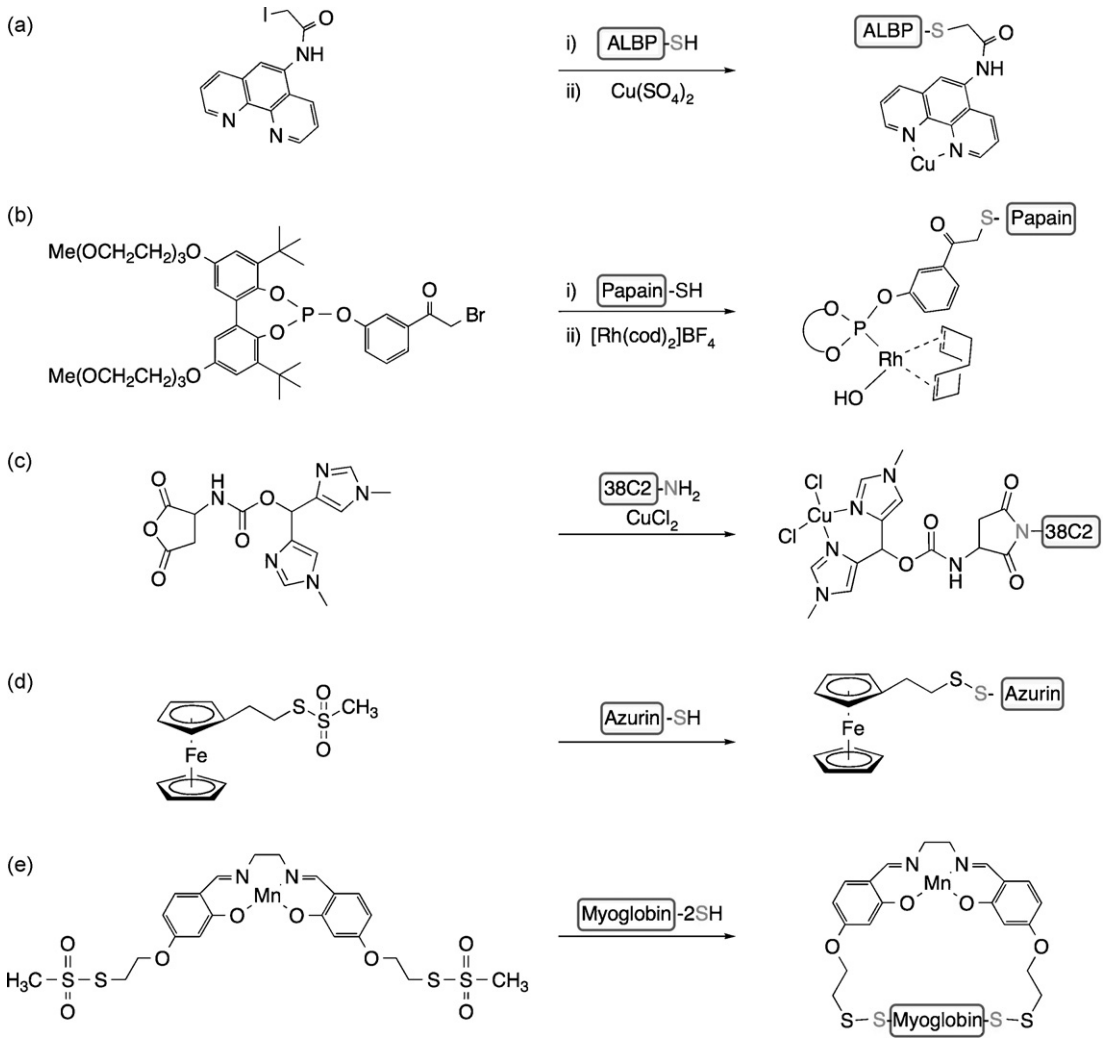

Fig. 3. Various covalent strategies for introduction of metal complexes into protein scaffolds by haloacetyl derivatives (a and b), a bis-imidazoyl aspartic acid anhydride derivative (c), and methane thiosulfonate derivatives (d and e).

sists of 60 copies of two different types of protein subunits as 30 nm-diameter icosahedra (Fig. 2e). The particle is remarkably stable; it maintains its integrity at 60 °C (pH 7) for at least 1 h and in pH range from 3.5 to 9 at room temperature. Cowpea Chlorotic mottle virus (CCMV) is composed of 180 identical coat protein subunits arranged on an icosahedral lattice having an inner cavity of 18 nm in diameter [83]. Access of small molecules into the cage is regulated by reversible pH-dependent swelling which results in a 10% increase in virus dimension [83]. Huge supramolecular assemblies such as tobacco mosaic virus [84–87], M-13 bacteriophage [63,88,89] S-layer protein [90], and chaperonins [91,92] have also been reported to give vacant space for the deposition of metal materials.

2.2. Covalent insertion of unnatural metal cofactors

Covalent cross-linkage is an attractive approach to conjugate metal complexes to specific sites of protein scaffolds directly [31]. Davies and Distefano have reported modification of a cysteine residue of an adipocyte lipid binding protein (ALBP) with a 1,10-phenanthroline derivative in their pioneer work (Fig. 3a) [93]. The modified protein can specifically capture a Cu(II) cation. Similar strategy was also applied for the introduction of an organometal complex into a protein scaffold of papain (Fig. 3b) [94]. Phosphorus donor ligands are essential to prepare many organometal complexes that catalyze many reactions. A bromoacetoamido derivative of a phosphorus ligand was attached to Cys25 located at the hydrophobic active site of papain. After the reaction of the modified papain and a Rh(cyclooctadiene) complex, the conjugate formation was confirmed by ESI MS [94].

Janda and co-workers have applied a covalent method to the construction of novel metallo-antibodies containing synthetic cofactors (Fig. 3c) [95]. They selected antibody 38C2 having a highly nucleophilic low-pK_a lysine residue in a hydrophobic pocket [95–97]. The lysine residue could selectively react with a bis-imidazoyl aspartic acid anhydride derivative. The resulting hybrid antibody captured one Cu ion at the synthetic binding site.

Lu et al. have reported the use of active sites of metalloproteins for cross-linking of metal complexes (Fig. 3d and e) [41,98]. Blue copper azurin (Az), which is an electron transfer

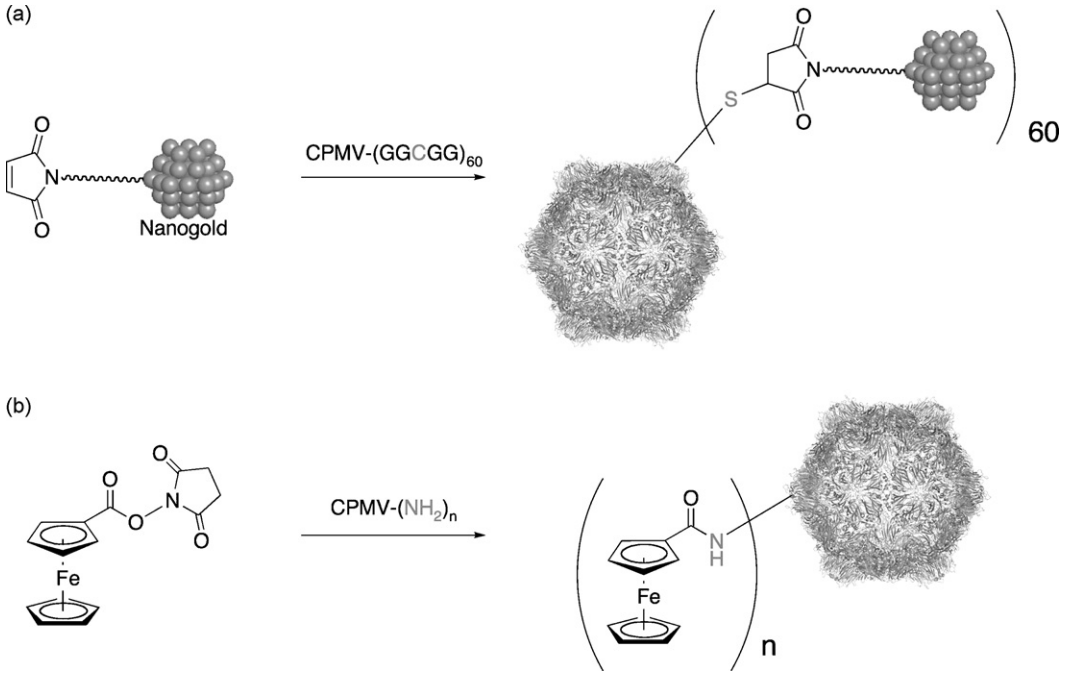

Fig. 4. Covalent conjugations of gold nanocluster (a) and Fc (b) on the CPMV surface.

protein, holds a copper atom at the active site by coordination of two histidines, one methionine, and one cysteine. The cys residue was utilized to load a ferrocene (Fc) derivative by the reaction of a cysteinyl thiol and a thiosulfonate derivative [98]. They have also developed a unique method to anchor a metal complex tightly in a metalloprotein scaffold [41]. For this purpose, Lue72 in the Mb active site was replaced with a cysteine residue by site-directed mutagenesis. Furthermore, they introduced one additional cysteine residue into the position 103 to conjugate with dual anchoring of a Mn^{III}(Schiff base) complex having two thiosulfonate moieties. They intended precise control of the placement of the metal complex with specific orientation and limited rotational freedom.

The CPMV virus cage also shows unique properties for covalent conjugations (Fig. 4). Finn et al. have displayed 60 gold nanoparticles on the icosahedral cage surface by the modification of cysteine residues with nanogold tethering to a maleimide group (Fig. 4a) [79]. Although there is no cysteine residue on the surface, a cysteine containing fragment (Gly-Gly-Cys-Gly-Gly) was inserted between the positions 98 and 99, which are located on the exterior surface of the large subunit. Thus, 60 cysteinyl thiols are exposed on the surface of CPMV and readily modified by various reagents. In addition, lysine residues located on the surface of CPMV can be used as platforms of the covalent cross-linking of metal complexes and materials [66,99]. Wild type CPMV has five lysine residues on the solvent exposed exterior of each of 60 asymmetric units. These lysine residues were treated with Fc *N*-hydroxysuccinimidyl esters and the attachment of 240 Fc moieties was confirmed (Fig. 4b) [66]. Moreover, two most reactive lysine residues were created as attachment sites by replacing all other lysine residues [99]. The mutants show the selective conjugation with gold nanoparticles.

2.3. Non-covalent insertion of unnatural metal cofactors

There are a series of papers on the non-covalent insertion of metal cofactors using (i) metal complex anchored to native substrates, (ii) modified metal cofactors, and (iii) synthetic metal complexes [24,28,29]. Although the former two methods are very convenient to introduce many functions into proteins, there is limitation in type of proteins and synthesis of modified substrates and cofactors. If synthetic metal compounds, whose structures are very different from the native cofactors, can be introduced into protein cages as simple as the heme prosthetic group that is non-covalently bound in the cavity of heme proteins, the bio-conjugation of metal complexes will be applicable to many proteins and metal complexes. Thus, we have developed a new method for the preparation of metal complexes placed in protein cavities by non-covalent fixation (method (iii)).

The first example of the method (i) was reported by Wilson and Whitesides in the 1970s [5]. They synthesized a diphosphine ligand conjugated with a biotin molecule to introduce a Rh(norbornadiene) catalyst into the avidin active site. Recently, the method was applied to various organometal complexes by Ward and co-workers (Fig. 5a) [26,29,42–44,100]. Furthermore, metal complexes containing a modified enzyme inhibitor as a ligand can bind to the target proteins [6,9,53,101]. The organometal moieties of the compounds make the composite stable by non-covalent interactions with the surrounding amino acid residues.

Heme modification is an example of the method (ii) [28,36]. Two propionic acids of heme are the candidates for the covalent attachment of functional groups to heme. Hayashi and co-workers have reported a charged heme [37], glycosylated heme [102], and flavohemin [33] for the reconstitution of them with apo-Mb (Fig. 5b).

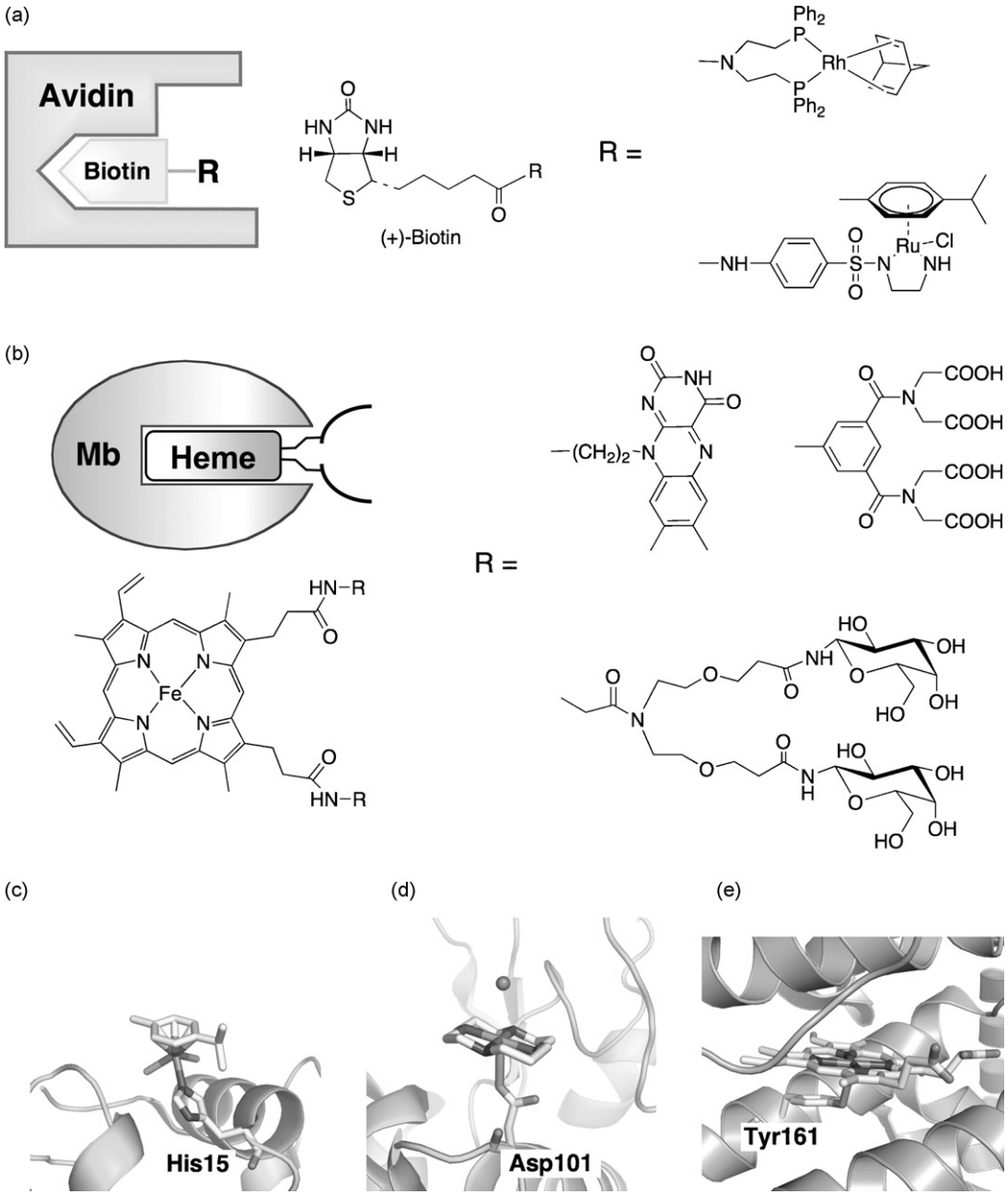

Fig. 5. Non-covalent insertion of metal complexes to protein vacant space by modifying biotin (a) and heme (b), ligation to amino acid residues (c–e).

In the case of the method (iii), coordination of metal complexes to amino acid residues is a crucial factor to stabilize the metal complex/protein composites. Sadler and co-workers have reported the crystal structures of ruthenium half-sandwich complex/lysozyme and copper-cyclams/lysozyme composites [8,9]. These structures showed the Ru and Cu atoms coordinating to His15 and Asp101, respectively, to stabilize unusual configuration (Fig. 5c and d) [8,9]. The crystal structure of HAS–hemin composite also reveals that Tyr161 ligates to the iron atom of hemin (Fig. 5e) [13].

We have employed apo-Mb and metal(Schiff base) complexes in preparing hybrid metalloproteins by the method (iii) (Scheme 1) [15,16,24,39]. Apo-Mb has a cavity of *ca.* 10 Å diameter to accommodate heme (Fig. 2b). The heme is bound to His93 and stabilized by non-covalent interactions with adjacent amino acid residues [72]. Advantage of Schiff base complexes for the heme substitution is that their molecular size and coordination geometry are almost identical to those of heme and it is easy to modify the ligand size and hydrophobicity. Schiff base complexes having high affinity for apo-Mb and apo-Mb mutants were screened by using ESI-TOF MS [16,24,39]. Thus, ESI-TOF MS has been routinely used to determine relative binding affinity between biomolecules and metal complexes [103]. In order to compare the affinity of a series of Fe^{III}(Schiff base) complexes with apo-Mb, competitive reconstitution was employed. For example, the mass spectrum of a mixture of **Fe·1**, **Fe·2**, **Fe·3** and apo-Mb gave three peaks corresponding to **Fe·1**·, **Fe·2**·, and **Fe·3·apo-Mb**, and relative peak intensity of each composite is in the order of **Fe·2** > **Fe·1** > **Fe·3** as shown in Fig. 6. The same order of stability was observed for the melting temperature (T_m) of

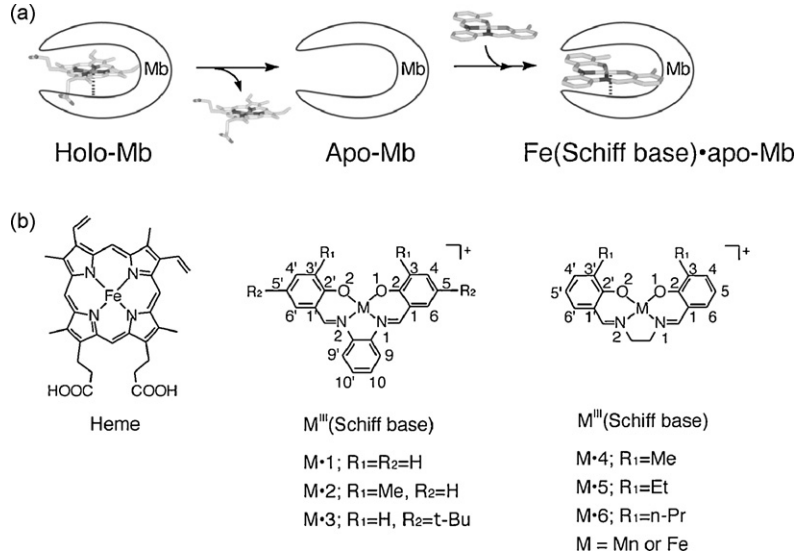

Scheme 1. Typical preparation scheme of Schiff base complex/apo-Mb composites (a) and molecular structures of heme and Schiff base complexes (b).

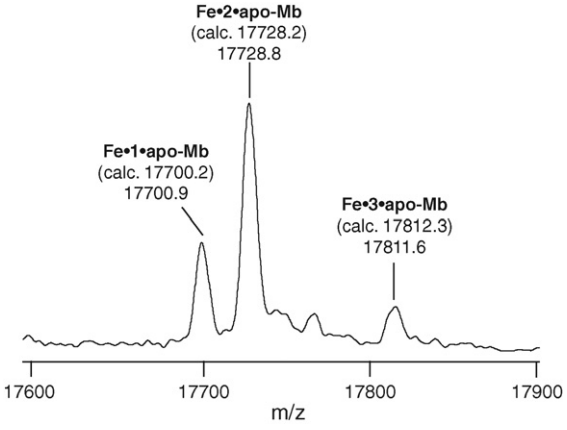

Fig. 6. The ESI-TOF MS spectrum of apo-Mb reconstituted by a mixture of **Fe·1**, **Fe·2**, and **Fe·3**. Concentrations of **Fe·1**, **Fe·2**, **Fe·3**, and apo-Mb were 10, 10, 10, and 30 μM, respectively [16].

them determined by circular dichroism (CD) spectral measurements at various temperatures. The results suggest that methyl groups at the 3 and 3′ positions in **Fe·2** are effective on the binding affinity. Thus, we have designed an apo-Mb mutant suitable for the fixation of Schiff base complexes in the apo-Mb active site by using Insight II/Discover 3. The calculation results suggest that the alanyl side chain at the position 71 in apo-Mb is expected to sterically interact with the Schiff base ligands if the complex coordinates to His93 as observed for heme. Thus, Ala71 was replaced to Gly in order to improve the binding affinity of the complexes in the active site.

The crystal structure of **Fe·2·apo-A71GMb** shows that the iron complex **Fe·2** is fixed in the heme cavity of apo-A71G Mb (Fig. 7a). The N^{ε} atom of proximal His93 ligates to the heme iron with a Fe–N distance of 2.30 Å, consistent with the model calculations. The orientation of **Fe·2** in the cavity of apo-A71GMb is constrained by several specific interactions with Phe43, Leu89, His97 and Ile99 which are close *to* **Fe·2** within the distances of π–π and CH–π interactions (Fig. 8) [104]. The side chain of Ile107 is located between the 3- and 3′-methyl groups of **Fe·2**. At the same time, the C5 atom is close to the Cα atom of Ala71Gly with a distance of 3.95 Å as shown in Fig. 8. On the other hand, the **Fe·2·apo-Mb** structure is problematic, while it provides useful insights into the nature of the binding of **Fe·2**. The protein portion in the crystal structure of **Fe·2·apo-Mb** is well defined and it is similar to that of native met-Mb

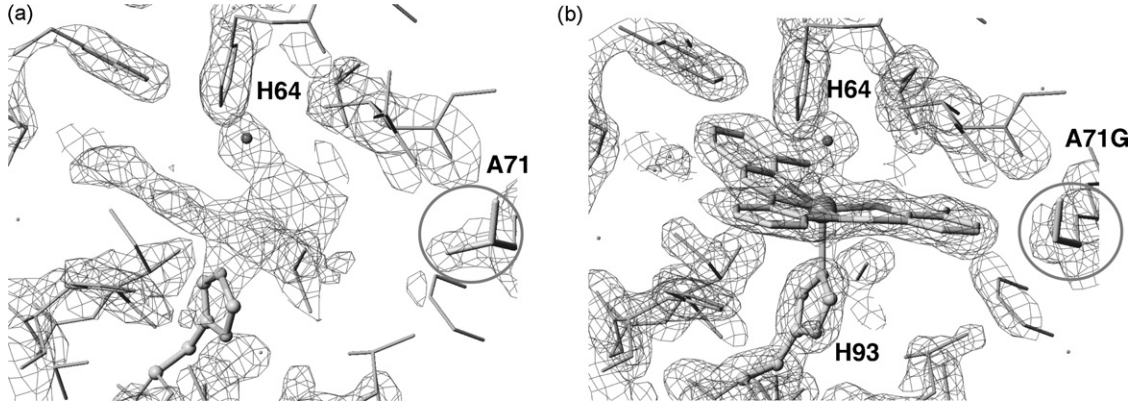

Fig. 7. The electron-density maps of **Fe·2·apo-A71GMb** (a) and **Fe·2·apo-Mb** (b). The final models are superimposed on the maps [16].

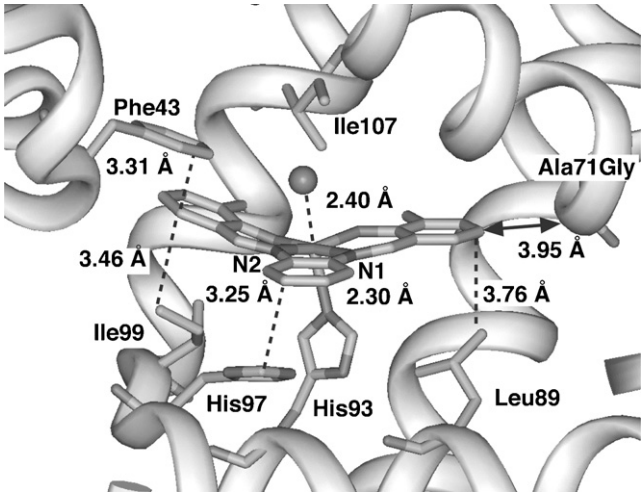

Fig. 8. The active site structure of **Fe·2·apo-A71GMb** [16].

(RMSD = 0.68 Å). While His64 and Ala71, which are close to **Fe·2**, are clearly defined, the electron density of the 3,3′-Me_2-salophen ligand and the iron atom appear to be distributed in the cavity (Fig. 7b). The results suggest that **Fe·2** and the ligated imidazole of His93 are moving around in apo-Mb or take several conformations.

2.4. Deposition of metal cations and nanoparticles

Metal cations can be deposited on (i) the interior surface of proteins such as apo-Fr [54,55,75,78,105] or (ii) metal-binding peptide fragments introduced to protein cages [55,61–64,106]. Nanoparticles are also prepared by (iii) encapsulation of them in protein cages [47,65]. Apo-Fr is stable at high temperature, even it contains metal cations, such as Co, Cu, Zn, Pd, Cd, and so on. Fr containing those metal ions is applied to mineralization of them to metal sulfide, metal oxide, and zero-valent metal particles by self-assembly, oxidation, and reduction, respectively. For the method (ii), some polypeptide sequences exhibiting affinity for various inorganic materials have been selected by phage and cell-surface display [106]. Naik et al. prepared a Fr mutant containing dodecapeptide fragments that reduce silver cations to metallic silver (Fig. 9a) [55,107]. Belcher's peptide having high affinity to the L10 phase of CoPt nanoparticles was introduced inside of the heat shock protein (Hsp) cage (Fig. 9b) [62,63]. The CoPt particle prepared in the cage exhibits magnetic properties of 150 and 610 G before and after annealing [62]. Viral cages have positively charged interiors to stabilize polyanion charge of RNA. In order to deposit iron cations on the interior surface of the CCMV cage, the positive charge region was changed to negative one by alternation of nine basic residues at the N-terminal with glutamic acid [64]. The resulting CCMV can uptake Fe(II) cations and convert them to single mineralized-crystal of γ-FeOOH [64]. Native and synthetic histidine-rich peptides having high affinity for metal ions and nanoclusters have also been used to control the nanoparticle patterning and size distribution of nanoclusters [108]. We have reported the construction of a tetrapod assembly of four bio-nanotubes of gene product 5(gp5) (Fig. 9c) [109], a component of bacteriophage T4 [110], by *in situ* formation of Au nanocluster [108], i.e., a His-tag fragment was introduced at the C-terminal of gp5 to assemble the ordered tetrapod-like composite around a Au nanocluster. On the other hand, gold or quantum dot particles modified by RNA/DNA or negatively charged polymers were encapsulated in viral capsids using coat-protein self-assembly [65,111].

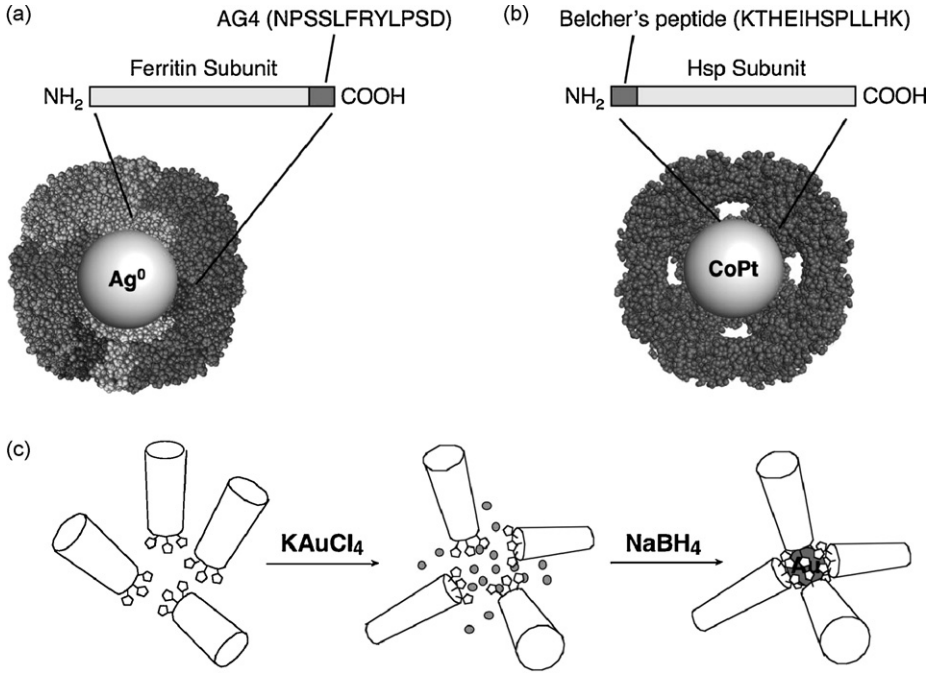

Fig. 9. Preparations of metal nanoparticles by using peptide fragments having high affinity to Ag^0 (a), CoPt (b) and Au^0 (c).

3. Functions of artificial metalloproteins

3.1. Catalytic properties

Improvement of activity and selectivity in catalytic reactions are very important subjects for the construction of artificial metalloenzymes. Although there are many reports on bio-conjugated metal complexes or materials with proteins [29,32,105], it is still difficult to improve catalytic activity and selectivity of artificial enzymatic reactions.

Lu et al. have applied the two-point covalent attachment strategy for the introduction of a synthetic metal cofactor into apo-Mb to enhance enantioselective sulfoxidation [41]. They introduced a Mn(salen) complex into the apo-Mb Y103C mutant by the cross-linking of a methane thiosulfonate group in the complex. However, the activity and enantioselectivity of thioanisole sulfoxidation remained low (51×10^{-3} turnover min^{-1}, 12% ee (*S*)) possibly due to Mn(salen) being located at the active site with multiple orientations. When the dual cross-linking sites, L72C and Y103C were introduced to limit the conformational freedom, significant increases in the rate and ee% were observed (390×10^{-3} turnover min^{-1}, 51% ee (*S*)) (Fig. 10a).

The non-covalent strategy is a powerful tool for the construction of artificial metalloproteins and combinatorial screening can be applicable to identify the optimized metal cofactors. Ward et al. have used a chemogenetic-optimization procedure to search the best synthetic metal cofactor/protein combination for enantioselective reactions [26,42–44]. They prepared 20 streptavidin mutants using saturation mutagenesis at the position 112. Their enzyme library contains 360 artificial metalloproteins afforded by combination of the resultant 20 proteins and 18 biotinylated metal complexes. Finally, they found the best artificial transfer hydrogenase to afford the product with up to 97% ee (*R*) (Fig. 10b) [26].

Reetz et al. have applied directed evolution to the enhancement of the enantioselective olefin hydrogenation by a biotinylated Rh complex anchored to streptavidin [27]. They utilized a CASTing method to replace appropriate amino acid residues close to the active site by saturation mutagenesis [112]. At first, they selected four replacing sites using a model calculation based on the crystal structure of the streptavidin–biotin complex. The first generation of saturated mutation at Ser112 indicated that the Ser112Gly mutant catalyzes the reaction with 35% ee (*R*). Then, they attempted iterative CASTing of the mutant Ser112Gly at the position 49. The Asn49Val/Ser112Gly showed 54% ee (*R*) in the reaction. Finally, the third generation in the saturation experiment of the double mutant at the position 112 showed that the mutant Asn49Val catalyzes the reaction with 65% ee (*R*).

Table 2
Enantioselective thioanisole sulfoxidation[a]

Catalyst	Rate[b]	% ee
Mn·4·apo-A71GMb	1295 ± 119	17 ± 0.6 (*S*)
Mn·5·apo-A71GMb	803 ± 5	23 ± 0.2 (*S*)
Mn·6·apo-A71GMb	2724 ± 69	27 ± 0.1 (*S*)
Mn·1·apo-H64D/A71GMb	158 ± 8	23 ± 0.5 (*R*)
Mn·4·apo-H64D/A71GMb	464 ± 62	32 ± 0.1(*R*)
Mn·5·apo-H64D/A71GMb	135 ± 5	5 ± 0.7 (*R*)
Mn·6·apo-H64D/A71GMb	180 ± 7	13 ± 0.5 (*S*)
Mn·4 in buffer	62 ± 3	0
Mn·5 in buffer	39 ± 6	0
Mn·6 in buffer	87 ± 6	0

[a] Sulfoxidation was carried out in sodium acetate buffer (50 mM, pH 5.0) at 35 °C in the presence of a Mb composite (10 μM), thioanisole (1 mM), and H_2O_2 (1 mM) [15,39].
[b] The unit of the rate is 10^{-3} turnover min^{-1}.

We have designed Schiff base ligands to improve their catalytic oxidation activity in the apo-Mb cavity on the basis of their crystal structures [15]. The crystal structure of **Mn·2·apo-A71GMb** shows a narrow channel between His64 and the phenylenediamine unit of 2. Thus, they were replaced with Asp and an ethylenediamine unit, respectively, to enlarge the active site. The H_2O_2-dependent sulfoxidation of thioanisole was examined at 35 °C (50 mM sodium acetate buffer, pH 5.0) and the results are listed in Table 2. Mn(salen derivative)·apo-A71GMbs show 21–31-fold increased rates than those of Mn(salen derivative) in the same buffer solution (Table 2). In addition, we have designed an enlarged cavity by the replacement of **2** with **4** to increase the accessibility of substrates. The rate with **Mn·4·apo-H64D/A71GMb** is threefold higher than that with **Mn·2·apo-H64D/A71GMb**.

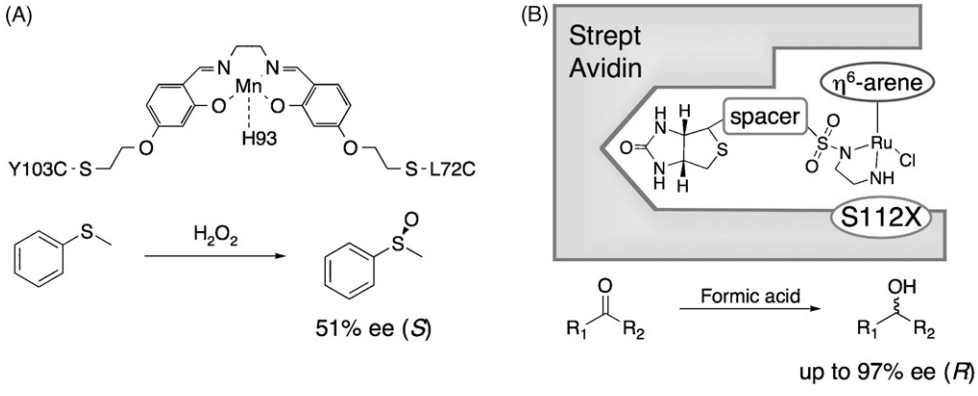

Fig. 10. Schematic drawings of asymmetric sulfoxidation and transfer hydrogenation using Mn(Schiff base)/apo-Mb (a) and Ru(arene)-biotin/streptavidin (b), respectively.

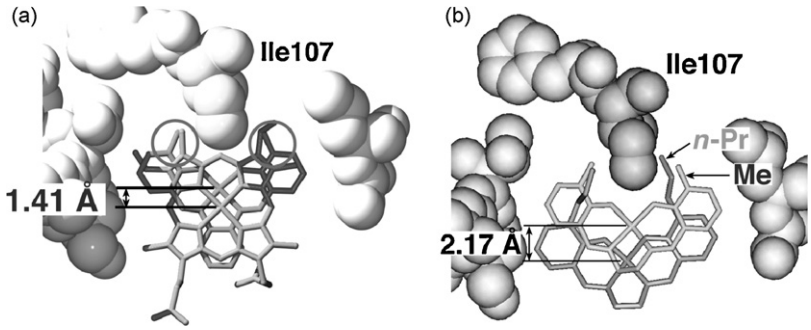

Fig. 11. The active site structure of **Mn·2·apo-A71GMb** superimposed on wild-type Mb (a) and calculated structure of **Mn·4·apo-H64D/A71GMb** superimposed on **Mn·6·apo-H64D/A71GMb** (b). The calculations were performed with InsightII/Discover 3 using the ESFF force field.

The crystal structure of **Mn·2·apo-A71GMb** shows a hydrophobic interaction between the 3- and 3′-methyl groups and Ile107 (Fig. 11a). As discussed before, the replacement of the methyl groups with bulkier ethyl and *n*-propyl groups is expected to change the position of the metal ion. Molecular modeling calculation of Mn(3,3′-X_2-salen)·apo-H64D/A71GMbs (X = Me, Et, and *n*-Pr) indicates that the Mn atoms of **Mn·5** and **Mn·6** in the protein could locate 0.83 and 2.17 Å outside from the position of **Mn·4**, respectively (Fig. 11b). In addition, the calculation suggests that the position of thioanisole in the active site is not changed since the replacement of two methyl groups with Et or *n*-Pr does not affect the interaction of the phenyl group in thioanisole with Phe43 and Leu32. These considerations indicate that the relative position of the sulfur atom and the oxo-metal center could be altered to result in the change of enantioselectivity in the sulfoxidation. While **Mn·4·apo-H64D/A71GMb** showed 32% ee (*R*) selectivity, introduction of bulkier groups at the 3,3′-positions induces relative *S*-selectivity to end up 13% (*S*) for **6**.

3.2. Electrochemical properties

Fundamental understanding and application of redox reactions concerning inter- and intra-protein electron transfer (ET) are very important subjects in bioinorganic chemistry. For example, Winkler and Gray have studied the ET mechanism of Ru-modified proteins [113]. However, it is still challenging to utilize a protein–protein ET system to reductively activate artificial cofactors introduced in proteins due to lack of understanding on interactions between the cofactor and the system contributing to ET.

Redox property of Fc was changed in a protein cavity [98]. Upon the attachment of Fc to the active site of blue copper azurin (Az) with the covalent conjugation, Fc–Az showed a midpoint redox potential (E_m) of 579 mV (versus normal hydrogen electrode (NHE)), while that of Fc is 402 mV. The positive shift was induced by hydrophobic environment around Fc (Fig. 12a). In addition, reversibility of CV of Fc–Az is higher than that of Fc without the conjugation to Az. This indicates increased stability of the ferrocenium ion in the protein scaffold. The composites can be used as a redox active agent of ferri-cyt *c*. The composite could be a potent building block of biosensors and biological ET studies.

Gray et al. synthesized ruthenium sensitizer-linked substrates for investigating biological reactions [51,113–116]. Ruthenium complexes served as rapid optical redox triggers for the reduction of cytochrome P450 camphor ($P450_{cam}$). A Ru-diimine moiety is conjugated with a substrate (adamantane) or a heme ligand (imidazole) using a perfluorinated biphenyl bridge [116,117]. The redox property of the sensitizer is controlled by the modification of the ligand of the Ru complex. The crystal structure of $P450_{cam}$ including the Ru sensitizer-linked substrate showed that an open conformation of the enzyme to fix the substrates in the 22 Å deep channel [19,117]. The composite proceeded an ET reaction from Ru to heme with a through-bond electronic coupling (Fig. 12b) [116]. The redox reaction is 5×10^5 faster than the biological reduction from putidaredoxin to heme [118].

For the construction of an artificial protein–protein ET system [37,116,119], we have employed heme oxygenase (HO) which catalyzes the conversion of heme to biliverdin [17]. In the catalytic cycle of the enzymatic reaction, HO receives two electrons from NADPH-cytochrome P450 reductase (CPR) by making a protein–protein complex [120]. We attempted to reduce Fe^{III}(Schiff base), instead of heme, located at the active site of HO by NADPH-CPR (Fig. 13a). This reaction was accelerated when the Schiff base complex having a carboxylate group capable to form the hydrogen bond conserved between heme and HO was used, though E_m of the hydrogen bonding **Fe·7·HO** (−76 mV versus NHE) is lower than that of an unmodified **Fe·1·HO** composite (+15 mV versus NHE). Crystal structures of human [121], rat [122] and *Corynebacterium diotheriae* [123] HOs show an invariant hydrogen bond between the guanido N^{η} atom of Arg177 (Arg183 in human and rat HO) and the O atom of heme propionate-7. The mutagenesis experiments concluded that this residue is one of the important residues for the formation of a transient ET complex with CPR [124]. Thus, when **heme·HO** makes a complex with CPR, Arg177 (in particular, the exposed N^{η} atom) is expected to have dual roles in both binding and ET with CPR as suggested for Arg112 in P450cam [125]. We succeeded in determining crystal structures of **Fe·l**, **Fe·7**, and **Fe·8·HO** [17]. In the case of **Fe·7·HO**, **Fe·7** has the same hydrogen bond with Arg177 (Fig. 13b) as observed for heme·HO, indicating that **Fe·7** is capable of receiving electron from CPR. On the other hand, Arg177 in **Fe·8·HO** is not in the position to assist the ET because one oxygen atom of

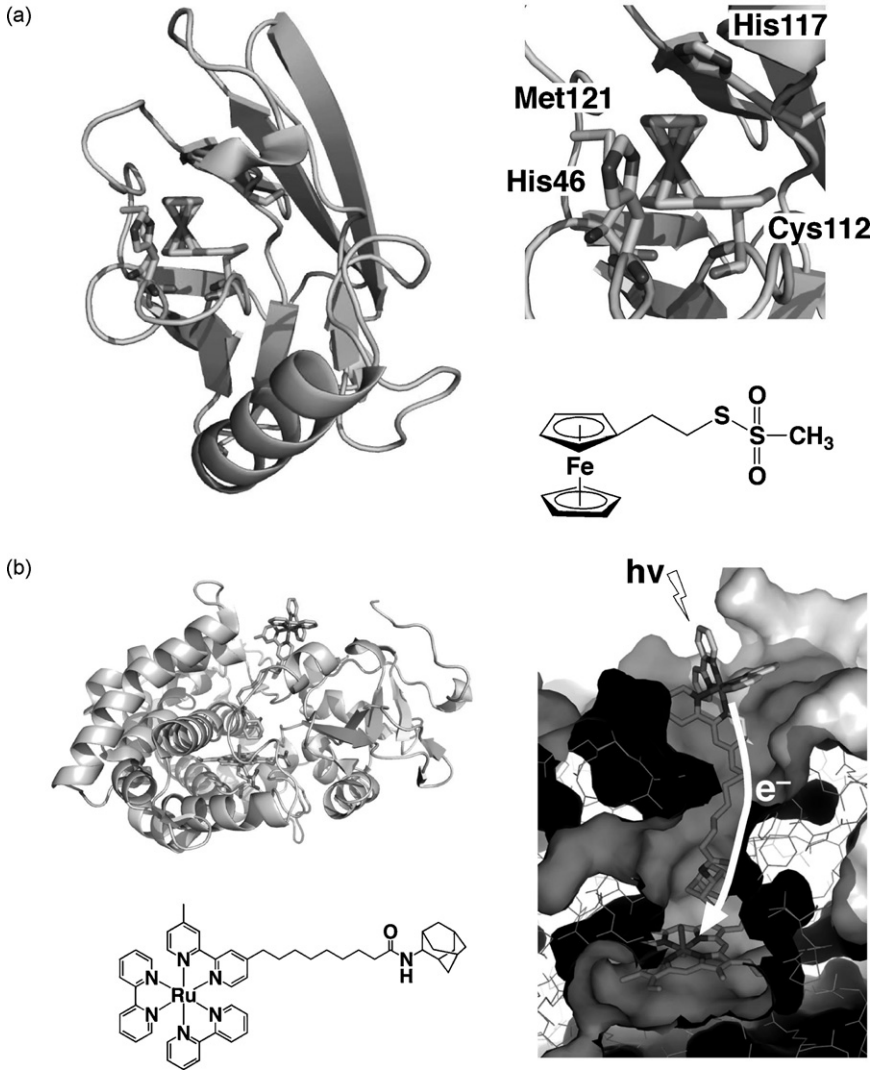

Fig. 12. A proposed structure of Fc–Az (a) and the crystal structure of $P450_{cam}$ including the Ru sensitizer-linked substrate (b) (PDB ID: 1QMQ).

the carboxyl group in **Fe·8** forms two hydrogen bonds with $N^{\eta 1}$(Arg177) and O^{η}(Tyr130). Further, **Fe·l** has no hydrogen bond with Arg177. Thus, Arg177 in **Fe·8·HO** and **Fe·1·HO** is expected to show less effect on the ET reaction with CPR. In fact, the reduction rate of the composites with NADPH-CPR depends on their hydrogen bonding interaction while the reduction rates of them by $Na_2S_2O_4$ are reasonably dependent on their redox potentials. These results suggest that the hydrogen bonding network of Arg177 and the propionate in **Fe·7** directly participates in the ET reaction of the HO/NADPH-CPR system. This is the first example of a synthetic metal complex activated through a protein–protein ET system, and showing that the hydrogen bond is also crucial in ET reactions of metalloproteins [126,127].

3.3. Material functions

A number of proteins with a diverse range of structures have been employed as frameworks for the construction of multidimensional devices, since they are useful materials for the deposition of metal nanoparticles and the mineralization of metal ions [128]. Fr is one of the most attractive protein cages for nanoreactors to provide unique functions and versatile nanoscale architectures [68]. However, difficulties in utilizing the composite materials for chemical reactions remain. We have reported *in situ* preparation of zero-valent palladium clusters by chemical reduction of palladium ions in the apo-Fr cage and its catalytic reactions (Fig. 14a) [54]. The palladium cluster is monodispersed (2.0 ± 0.3 nm) due to the preparation of the cluster in the size-restricted Fr interior. More importantly, the palladium clusters can catalyze size-selective olefin hydrogenation because substrates must penetrate into the Fr cavity through the size-restricted channels. In addition, the turnover frequency of acrylamide hydrogenation is 33,000/Pd·apo-Fr/hr under 1 atm H_2 atmosphere at 7 °C. This is the first example of catalytic reactions by synthetic metal clusters encapsulated in biomolecular assemblies.

Douglas et al. prepared a hybrid Fr cage for the use in cell-targeting cancer therapy [59,76,78,129]. As a cancer cell-targeting ligand, RGD-4C peptide was genetically incorporated at the N-terminal of heavy-chain ferritin (HFr) because the

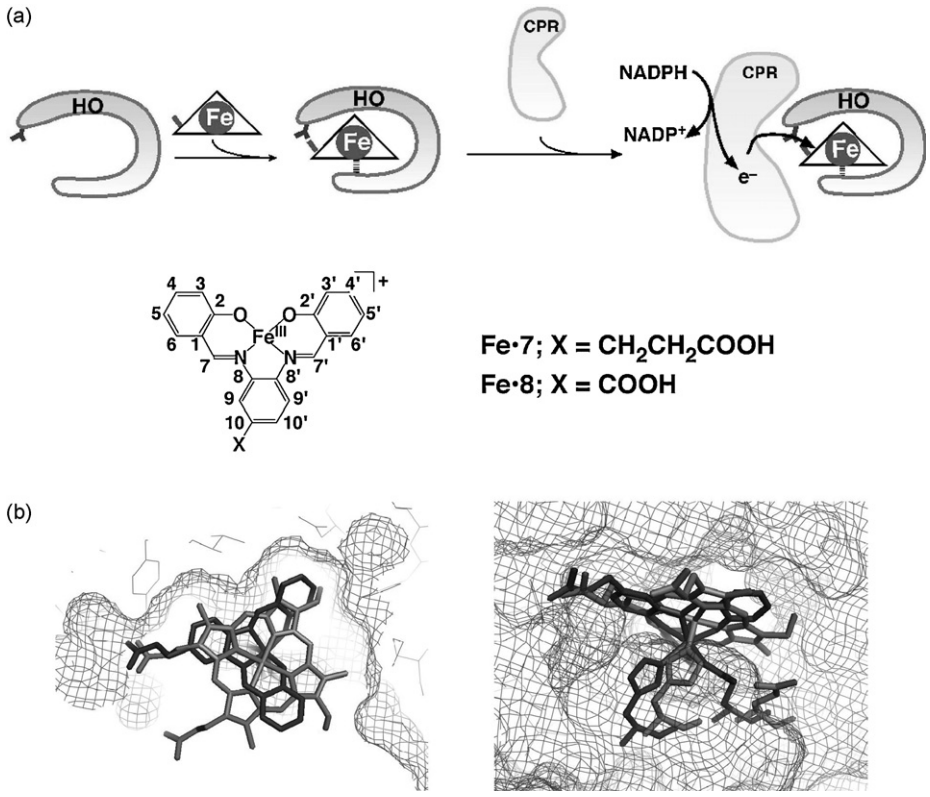

Fig. 13. Preparation of a Fe(Schiff base)·HO composite and the ET reaction from CPR and NADPH (a). Top and side views of the active site of **Fe·7·HO** superimposed on **heme·HO** (b).

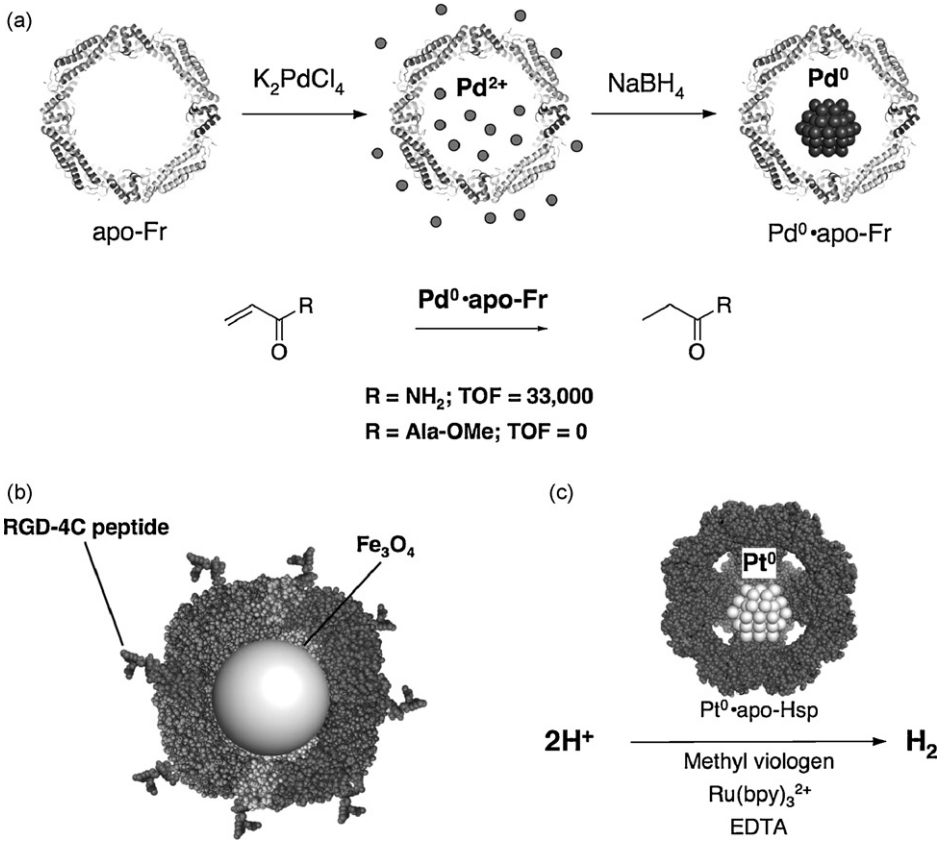

Fig. 14. Schematic drawings of Pd^0·apo-Fr (a), Fe_3O_4·apo-RDG4C-Fr (b), Pt^0·apo-Hsp (c), and their catalytic reactions.

terminal is exposed to the exterior surface of HFr [78]. Iron oxide mineral prepared in the cage exhibited superparamagnetic behavior at room temperature. Cell-targeting ability of the composite was estimated by the binding to C32 amelanotic melanoma cells [130]. Transmission electron microscopic images of the incubated sample of the cell and the RGD4C-Fr containing iron mineral clusters showed small electron-dense particles on the surface of the cells, corresponding to the mineral core in the Fr cages. The experiment demonstrated cell-targeting derivatives by using multifunctional protein container (Fig. 14b).

A biomimetic material aimed for artificial hydrogenase was synthesized by employing small heat shock protein (Hsp) [131]. The native enzyme produces hydrogen from a renewable source such as solar energy [132]. Varpness et al. prepared Pt particles in the protein cage. The composite catalyzes the hydrogen production in the presence of EDTA, Ru(2,2′-bipyridine)$_3^{2+}$, methyl viologen as a reductant, photocatalyst, and electron-transfer mediator (Fig. 14c) [131]. The system in the protein cage architecture can provide a new concept for hydrogen production.

4. Summary

Great progress for the preparation of artificial metalloproteins has been made by combinatorial or genetical screening approaches for the last several years. Unnatural metal cofactors and materials have been designed to introduce them into small protein cavities as well as large protein cages such as viruses and Fr. These progresses are achieved by cooperation of molecular and structural biology and inorganic chemistry. By the introduction of cofactors, the original functions of proteins are dramatically changed and we could utilize them for biotechnology of sensing and catalysis. These first generation efforts toward designing artificial metalloproteins are followed by improvement of their functions by structure-based rational design. The structural information on the artificial metalloenzymes are crucial for the 2nd generation design, since the main subjects of the first generation of the artificial proteins were focused on the reconstitution of artificial metalloproteins. Our results described in this review also show a new method of non-covalent insertion of metal complexes instead of the typical covalent conjugations. More importantly, the results demonstrate that the enantioselectivity and catalytic activity of unnatural metal cofactors in protein cavities can be regulated by rational design of the cofactors based on crystal structures of the first generation composites. In addition, our method can be extended to various proteins and functions. For example, we have applied the method to protein–protein electron transfer systems and the utilization of a nanospace consisted of a protein assembly for activation and concentration of metal complexes, respectively. Furthermore, X-ray crystal structure analysis shows not only the coordination geometry of metal complexes and ions but also the dynamics of them in protein vacant spaces. For instance, the crystal structure of an artificial organometallic compound bound to a kinase allows us to elucidate inhibition mechanism of the kinase activity and design more potent metalloinhibitors [18]. The structures of several ferric ion-binding proteins containing a Hf cluster provide snapshots of dynamic coordination changes in protein assisted materials synthesis [10]. We believe that the results will provide intriguing implication on their applicable use for such as catalysts, sensors, metal drugs, and so on.

Acknowledgements

This work was supported by 21st Century COE program of Nagoya University for SA, and NY, Grant-in-Aid for Scientific Research (No. 18685019 for TU) and on Priority Areas (No. 16033226, “Chemistry of Coordination Space” for YW) from Ministry of Education, Culture, Sports, Science and Technology, Japan, and PRESTO, Japan Science and Technology Agency (JST).

References

[1] S.J. Lipard, J.M. Berg, Principle of Bioinorganic Chemistry, University Science Books, Mill Valley, CA, 1994.
[2] H.-B. Kraatz, N. Metzler-Nolte, Concepts and Models in Bioinorganic Chemistry, Wiley–VCH, Weinheim, 2006.
[3] S. Akabori, S. Sakurai, Y. Izumi, Y. Fujii, Nature 178 (1956) 323.
[4] H. Nozaki, S. Moriuti, H. Takaya, R. Noyori, Tetrahedron Lett. (1966) 5239.
[5] M.E. Wilson, G.M. Whitesides, J. Am. Chem. Soc. 100 (1978) 306.
[6] Y.K. Yan, M. Melchart, A. Habtemariam, P.J. Sadler, Chem. Commun. (2005) 4764.
[7] W.Q. Zhong, D. Alexeev, I. Harvey, M.L. Guo, D.J.B. Hunter, H.Z. Zhu, D.J. Campopiano, P.J. Sadler, Angew. Chem. Int. Ed. 43 (2004) 5914.
[8] I.W. McNae, K. Fishburne, A. Habtemariam, T.M. Hunter, M. Melchart, F.Y. Wang, M.D. Walkinshaw, P.J. Sadler, Chem. Commun. (2004) 1786.
[9] T.M. Hunter, I.W. McNae, X.Y. Liang, J. Bella, S. Parsons, M.D. Walkinshaw, P.J. Sadler, Proc. Natl. Acad. Sci. U.S.A. 102 (2005) 2288.
[10] D. Alexeev, H.Z. Zhu, M.L. Guo, W.Q. Zhong, D.J.B. Hunter, W.P. Yang, D.J. Campopiano, P.J. Sadler, Nat. Struct. Biol. 10 (2003) 297.
[11] V. Calderone, A. Casini, S. Mangani, L. Messori, P.L. Orioli, Angew. Chem. Int. Ed. 45 (2006) 1267.
[12] D.P. Barondeau, C.J. Kassmann, J.A. Tainer, E.D. Getzoff, J. Am. Chem. Soc. 124 (2002) 3522.
[13] P.A. Zunszain, G.J.T. Komatsu, E. Tsuchida, S. Curry, BMC Struct. Biol. 3 (2003) 6.
[14] M. Wardell, Z.M. Wang, J.X. Ho, J. Robert, F. Ruker, J. Ruble, D.C. Carter, Biochem. Biophys. Res. Commun. 291 (2002) 813.
[15] T. Ueno, T. Koshiyama, M. Ohashi, K. Kondo, M. Kono, A. Suzuki, T. Yamane, Y. Watanabe, J. Am. Chem. Soc. 127 (2005) 6556 (Throughout this reference, Refs. [24], and [39], assignments of *R*- and *S*-isomer of sulfoxide products are erroneously reversed. These assignments are corrected in this review).
[16] T. Ueno, M. Ohashi, M. Kono, K. Kondo, A. Suzuki, T. Yamane, Y. Watanabe, Inorg. Chem. 43 (2004) 2852.
[17] T. Ueno, N. Yokoi, M. Unno, T. Matsui, Y. Tokita, M. Yamada, M. Ikeda-Saito, H. Nakajima, Y. Watanabe, Proc. Natl. Acad. Sci. U.S.A. 103 (2006) 9416.
[18] J.E. Debreczeni, A.N. Bullock, G.E. Atilla, D.S. Williams, H. Bregman, S. Knapp, E. Meggers, Angew. Chem. Int. Ed. 45 (2006) 1580.
[19] I.J. Dmochowski, B.R. Crane, J.J. Wilker, J.R. Winkler, H.B. Gray, Proc. Natl. Acad. Sci. U.S.A. 96 (1999) 12987.
[20] B.R. Crane, A.J. Di Bilio, J.R. Winkler, H.B. Gray, J. Am. Chem. Soc. 123 (2001) 11623.
[21] A.M. Blanco-Rodriguez, M. Busby, C. Gradinaru, B.R. Crane, A.J. Di Bilio, P. Matousek, M. Towrie, B.S. Leigh, J.H. Richards, A. Vlcek, et al., J. Am. Chem. Soc. 128 (2006) 4365.
[22] S.M. Contakes, G.A. Juda, D.B. Langley, N.W. Halpern-Manners, A.P. Duff, A.R. Dunn, H.B. Gray, D.M. Dooley, J.M. Guss, H.C. Freeman, Proc. Natl. Acad. Sci. U.S.A. 102 (2005) 13451.

[23] A. Muller, A.J. Wilkinson, K.S. Wilson, A.K. Duhme-Klair, Angew. Chem. Int. Ed. 45 (2006) 5132.
[24] T. Ueno, T. Koshiyama, S. Abe, N. Yokoi, M. Ohashi, Y. Satake, H. Nakajima, Y. Watanabe, J. Organomet. Chem. 692 (2007) 142.
[25] M.A. Dwyer, L.L. Looger, H.W. Hellinga, Proc. Natl. Acad. Sci. U.S.A. 100 (2003) 11255.
[26] C. Letondor, A. Pordea, N. Humbert, A. Ivanova, S. Mazurek, M. Novic, T.R. Ward, J. Am. Chem. Soc. 128 (2006) 8320.
[27] M.T. Reetz, J.J.P. Peyralans, A. Maichele, Y. Fu, M. Maywald, Chem. Commun. (2006) 4318.
[28] T. Hayashi, Y. Hisaeda, Acc. Chem. Res. 35 (2002) 35.
[29] C.M. Thomas, T.R. Ward, Chem. Soc. Rev. 34 (2005) 337.
[30] Y. Lu, S.M. Berry, T.D. Pfister, Chem. Rev. 101 (2001) 3047.
[31] D. Qi, C.-M. Tann, D. Haring, M.D. Distefano, Chem. Rev. 101 (2001) 3081.
[32] Y. Lu, Angew. Chem. Int. Ed. 45 (2006) 5588.
[33] T. Matsuo, T. Hayashi, Y. Hisaeda, J. Am. Chem. Soc. 124 (2002) 11234.
[34] H. Sato, T. Hayashi, T. Ando, Y. Hisaeda, T. Ueno, Y. Watanabe, J. Am. Chem. Soc. 126 (2004) 436.
[35] T. Hayashi, H. Dejima, T. Matsuo, H. Sato, D. Murata, Y. Hisaeda, J. Am. Chem. Soc. 124 (2002) 11226.
[36] Y.-Z. Hu, S. Tsukiji, S. Shinkai, S. Oishi, I. Hamachi, J. Am. Chem. Soc. 122 (2000) 241.
[37] Y. Hitomi, T. Hayashi, K. Wada, T. Mizutani, Y. Hisaeda, H. Ogoshi, Angew. Chem. Int. Ed. 40 (2001) 1098.
[38] S. Neya, K. Imai, H. Hori, H. Ishikawa, K. Ishimori, D. Okuno, S. Nagatomo, T. Hoshino, M. Hata, N. Funasaki, Inorg. Chem. 42 (2003) 1456.
[39] M. Ohashi, T. Koshiyama, T. Ueno, M. Yanase, H. Fujii, Y. Watanabe, Angew. Chem. Int. Ed. 42 (2003) 1005.
[40] S.K. Ma, Y. Lu, J. Inorg. Biochem. 74 (1999) 217.
[41] J.R. Carey, S.K. Ma, T.D. Pfister, D.K. Garner, H.K. Kim, J.A. Abramite, Z. Wang, Z. Guo, Y. Lu, J. Am. Chem. Soc. 126 (2004) 10812.
[42] C. Letondor, N. Humbert, T.R. Ward, Proc. Natl. Acad. Sci. U.S.A. 102 (2005) 4683.
[43] G. Klein, N. Humbert, J. Gradinaru, A. Ivanova, F. Gilardoni, U.E. Rusbandi, T.R. Ward, Angew. Chem. Int. Ed. 44 (2005) 7764.
[44] M. Skander, N. Humbert, J. Collot, J. Gradinaru, G. Klein, A. Loosli, J. Sauser, A. Zocchi, F. Gilardoni, T.R. Ward, J. Am. Chem. Soc. 126 (2004) 14411.
[45] S. Crobu, M. Marchetti, G. Sanna, J. Inorg. Biochem. 100 (2006) 1514.
[46] M.T. Reetz, N. Jiao, Angew. Chem. Int. Ed. 45 (2006) 2416.
[47] A. Mahammed, Z. Gross, J. Am. Chem. Soc. 127 (2005) 2883.
[48] T. Komatsu, N. Ohmichi, P.A. Zunszain, S. Curry, E. Tsuchida, J. Am. Chem. Soc. 126 (2004) 14304.
[49] T. Komatsu, N. Ohmichi, A. Nakagawa, P.A. Zunszain, S. Curry, E. Tsuchida, J. Am. Chem. Soc. 127 (2005) 15933.
[50] M.L. Guo, H.Z. Sun, H.I. McArdle, L. Gambling, P.J. Sadler, Biochemistry 39 (2000) 10023.
[51] J. Zou, P. Taylor, J. Dornan, S.P. Robinson, M.D. Walkinshaw, P.J. Sadler, Angew. Chem. Int. Ed. 39 (2000) 2931.
[52] M.L. Guo, I. Harvey, D.J. Campopiano, P.J. Sadler, Angew. Chem. Int. Ed. 45 (2006) 2758.
[53] D.S. Williams, G.E. Atilla, H. Bregman, A. Arzoumanian, P.S. Klein, E. Meggers, Angew. Chem. Int. Ed. 44 (2005) 1984.
[54] T. Ueno, M. Suzuki, T. Goto, T. Matsumoto, K. Nagayama, Y. Watanabe, Angew. Chem. Int. Ed. 43 (2004) 2527.
[55] R.M. Kramer, C. Li, D.C. Carter, M.O. Stone, R.R. Naik, J. Am. Chem. Soc. 126 (2004) 13282.
[56] K.K.W. Wong, S. Mann, Adv. Mater. 8 (1996) 928.
[57] F.C. Meldrum, B.R. Heywood, S. Mann, Science 257 (1992) 522.
[58] K. Iwahori, K. Yoshizawa, M. Muraoka, I. Yamashita, Inorg. Chem. 44 (2005) 6393.
[59] S. Aime, L. Frullano, S.G. Crich, Angew. Chem. Int. Ed. 41 (2002) 1017.
[60] A.S. Blum, C.M. Soto, C.D. Wilson, J.D. Cole, M. Kim, B. Gnade, A. Chatterji, W.F. Ochoa, T.W. Lin, J.E. Johnson, et al., Nano Lett. 4 (2004) 867.
[61] J.M. Slocik, R.R. Naik, M.O. Stone, D.W. Wright, J. Mater. Chem. 15 (2005) 749.
[62] M.T. Klem, D. Willits, D.J. Solis, A.M. Belcher, M. Young, T. Douglas, Adv. Funct. Mater. 15 (2005) 1489.
[63] C.B. Mao, D.J. Solis, B.D. Reiss, S.T. Kottmann, R.Y. Sweeney, A. Hayhurst, G. Georgiou, B. Iverson, A.M. Belcher, Science 303 (2004) 213.
[64] T. Douglas, E. Stable, D. Willits, A. Aitouchen, M. Libera, M. Young, Adv. Mater. 14 (2002) 415.
[65] S.K. Dixit, N.L. Goicochea, M.C. Daniel, A. Murali, L. Bronstein, M. De, B. Stein, V.M. Rotello, C.C. Kao, B. Dragnea, Nano Lett. 6 (2006) 1993.
[66] N.F. Steinmetz, G.P. Lomonossoff, D.J. Evans Small, 2 (2006) 530.
[67] A. Messerschmidt, R. Huber, K. Wieghardt, T. Poulos, Handbook of Metalloproteins, vol. 1, Wiley, New York, 2001.
[68] A. Messerschmidt, R. Huber, T. Poulos, K. Wieghardt, Handbook of Metalloproteins, vol. 2, Wiley, New York, 2001.
[69] X.M. He, D.C. Carter, Nature 358 (1992) 209.
[70] G. Sudlow, D.J. Birkett, D.N. Wade, Mol. Pharmacol. 11 (1975) 824.
[71] T. Peters, All about Albumin: Biochemistry, Genetics and Medical Applications, Academic Press, San diego, 1995.
[72] C.L. Hunter, E. Lloyd, L.D. Eltis, S.P. Rafferty, H. Lee, M. Smith, A.G. Mauk, Biochemistry 36 (1997) 1010.
[73] E.A. Bayer, M. Wilchek, Meth. Enzymol. 184 (1990) 49.
[74] T. Douglas, D.P.E. Dickson, S. Betteridge, J. Charnock, C.D. Gamer, S. Mann, Science 269 (1995) 54.
[75] F.C. Meldrum, V.J. Wade, D.L. Nimmo, B.R. Heywood, S. Mann, Nature 349 (1991) 684.
[76] J.W.M. Bulte, T. Douglas, S. Mann, R.B. Frankel, B.M. Moskowitz, R.A. Brooks, C.D. Baumgarner, J. Vymazal, M.P. Strub, J.A. Frank, J. Magn. Reson. Imaging 4 (1994) 497.
[77] T. Douglas, V.T. Stark, Inorg. Chem. 39 (2000) 1828.
[78] M. Uchida, M. Flenniken, M. Allen, D. Willits, B. Crowley, S. Brumfield, A. Willis, L. Jackiw, M. Jutila, M. Young, et al., J. Am. Chem. Soc. 128 (2006) 16626.
[79] Q. Wang, T. Lin, L. Tang, J.E. Johnson, M.G. Finn, Angew. Chem. Int. Ed. 41 (2002) 459.
[80] A. Chatterji, W.F. Ochoa, T. Ueno, T. Lin, J.E. Johnson, Nano Lett. 5 (2005) 597.
[81] A.S. Blum, C.M. Soto, C.D. Wilson, T.L. Brower, S.K. Pollack, T.L. Schull, A. Chatterji, T.W. Lin, J.E. Johnson, C. Amsinck, et al., Small 1 (2005) 702.
[82] T.W. Lin, J.E. Johnson, Adv. Virus Res. 62 (2003) 167.
[83] T. Douglas, M. Young, Nature 393 (1998) 152.
[84] W. Shenton, T. Douglas, M. Young, G. Stubbs, S. Mann, Adv. Mater. 11 (1999) 253.
[85] C.E. Fowler, W. Shenton, G. Stubbs, S. Mann, Adv. Mater. 13 (2001) 1266.
[86] E. Dujardin, C. Peet, G. Stubbs, J.N. Culver, S. Mann, Nano Lett. 3 (2003) 413.
[87] R. Tseng, C. Tsai, L. Ma, J. Ouyang, C. Ozakan, Y. Yang, Nat. Nanotech. 1 (2006) 72.
[88] S.W. Lee, C.B. Mao, C.E. Flynn, A.M. Belcher, Science 296 (2002) 892.
[89] K.T. Nam, D.W. Kim, P.J. Yoo, C.Y. Chiang, N. Meethong, P.T. Hammond, Y.M. Chiang, A.M. Belcher, Science 312 (2006) 885.
[90] W. Shenton, D. Pum, U.B. Sleytr, S. Mann, Nature 389 (1997) 585.
[91] R.A. McMillan, C.D. Paavola, J. Howard, S.L. Chan, N.J. Zaluzec, J.D. Trent, Nat. Mater. 1 (2002) 247.
[92] D. Ishii, K. Kinbara, Y. Ishida, N. Ishii, M. Okochi, M. Yohda, T. Aida, Nature 423 (2003) 628.
[93] R.R. Davies, M.D. Distefano, J. Am. Chem. Soc. 119 (1997) 11643.
[94] L. Panella, J. Broos, J.F. Jin, M.W. Fraaije, D.B. Janssen, M. Jeronimus-Siratingh, B.L. Feringa, A.J. Minnaard, J.G. de Vries, Chem. Commun. (2005) 5656.
[95] K.M. Nicholas, P. Wentworth, C.W. Harwig, A.D. Wentworth, A. Shafton, K.D. Janda, Proc. Natl. Acad. Sci. U.S.A. 99 (2002) 2648.

[96] C.F. Barbas, A. Heine, G.F. Zhong, T. Hoffmann, S. Gramatikova, R. Bjornestedt, B. List, J. Anderson, E.A. Stura, I.A. Wilson, et al., Science 278 (1997) 2085.
[97] F. Tanaka, R.A. Lerner, C.F. Barbas, Chem. Commun. (1999) 1383.
[98] H.J. Hwang, J.R. Carey, E.T. Brower, A.J. Gengenbach, J.A. Abramite, Y. Lu, J. Am. Chem. Soc. 127 (2005) 15356.
[99] A. Chatterji, W.F. Ochoa, M. Paine, B.R. Ratna, J.E. Johnson, T.W. Lin, Chem. Biol. 11 (2004) 855.
[100] T.R. Ward, Chem. Eur. J. 11 (2005) 3798.
[101] U. Schaizschneider, N. Metzler-Nolte, Angew. Chem. Int. Ed. 45 (2006) 1504.
[102] T. Matsuo, H. Nagai, Y. Hisaeda, T. Hayashi, Chem. Commun. (2006) 3131.
[103] A. Kapur, J.L. Beck, S.E. Brown, N.E. Dixon, M.M. Sheil, Protein Sci. 11 (2002) 147.
[104] M. Nishio, M. Hirota, Y. Umezawa, The CH/π Interaction: Evidence, Nature, and Consequences, Wiley–VCH, New York, 1998.
[105] D.M. Vriezema, M.C. Aragones, J. Elemans, J. Cornelissen, A.E. Rowan, R.J.M. Nolte, Chem. Rev. 105 (2005) 1445.
[106] M. Sarikaya, C. Tamerler, A.K.Y. Jen, K. Schulten, F. Baneyx, Nat. Mater. 2 (2003) 577.
[107] R.R. Naik, S.J. Stringer, G. Agarwal, S.E. Jones, M.O. Stone, Nat. Mater. 1 (2002) 169.
[108] R. Djalali, Y.F. Chen, H. Matsui, J. Am. Chem. Soc. 125 (2003) 5873.
[109] T. Ueno, T. Koshiyama, T. Tsuruga, T. Goto, S. Kanamaru, F. Arisaka, Y. Watanabe, Angew. Chem. Int. Ed. 45 (2006) 4508.
[110] S. Kanamaru, P.G. Leiman, V.A. Kostyuchenko, P.R. Chipman, V.V. Mesyanzhinov, F. Arisaka, M.G. Rossmann, Nature 415 (2002) 553.
[111] L. Loo, R.H. Guenther, V.R. Basnayake, S.A. Lommel, S. Franzen, J. Am. Chem. Soc. 128 (2006) 4502.
[112] M.T. Reelz, M. Bocola, J.D. Carballeira, D.X. Zha, A. Vogel, Angew. Chem. Int. Ed. 44 (2005) 4192.
[113] J.R. Winkler, H.B. Gray, Chem. Rev. 92 (1992) 369.
[114] J.J. Wilker, I.J. Dmochowski, J.H. Dawson, J.R. Winkler, H.B. Gray, Angew. Chem. Int. Ed. 38 (1999) 90.
[115] M.J. Boerakker, N.E. Botterhuis, P.H.H. Bomans, P.M. Frederik, E.M. Meijer, R.J.M. Nolte, N. Sonunerdijk, Chem. Eur. J. 12 (2006) 6071.
[116] A.R. Dunn, I.J. Dmochowski, J.R. Winkler, H.B. Gray, J. Am. Chem. Soc. 125 (2003) 12450.
[117] A.R. Dunn, I.J. Dmochowski, A.M. Bilwes, H.B. Gray, B.R. Crane, Proc. Natl. Acad. Sci. U.S.A. 98 (2001) 12420.
[118] M.J. Hintz, D.M. Mock, L.L. Peterson, K. Tuttle, J.A. Peterson, J. Biol. Chem. 257 (1982) 4324.
[119] Y. Xiao, F. Patolsky, E. Katz, J.F. Hainfeld, I. Willner, Science 299 (2003) 1877.
[120] G.C. Chu, K. Katakura, X.H. Zhang, T. Yoshida, M. Ikeda-Saito, J. Biol. Chem. 274 (1999) 21319.
[121] D.J. Schuller, A. Wilks, P.R. Ortiz de Montellano, T.L. Poulos, Nat. Struct. Biol. 6 (1999) 860.
[122] M. Sugishima, Y. Omata, Y. Kakuta, H. Sakamoto, M. Noguchi, K. Fukuyama, FEBS Lett. 471 (2000) 61.
[123] S. Hirotsu, G.C. Chu, M. Unno, D.S. Lee, T. Yoshida, S.Y. Park, Y. Shiro, M. Ikeda-Saito, J. Biol. Chem. 279 (2004) 11937.
[124] J.L. Wang, P.R. Ortiz de Montellano, J. Biol. Chem. 278 (2003) 20069.
[125] M. Unno, H. Shimada, Y. Toba, R. Makino, Y. Ishimura, J. Biol. Chem. 271 (1996) 17869.
[126] D.S. Wuttke, M.J. Bjerrum, J.R. Winkler, H.B. Gray, Science 256 (1992) 1007.
[127] E. Babini, I. Bertini, M. Borsari, F. Capozzi, C. Luchinat, X.Y. Zhang, G.L.C. Moura, I.V. Kurnikov, D.N. Beratan, A. Ponce, et al., J. Am. Chem. Soc. 122 (2000) 4532.
[128] T. Douglas, M. Young, Science 312 (2006) 873.
[129] J.W.M. Bulte, T. Douglas, B. Witwer, S.C. Zhang, E. Strable, B.K. Lewis, H. Zywicke, B. Miller, P. van Gelderen, B.M. Moskowitz, et al., Nat. Biotechnol. 19 (2001) 1141.
[130] W. Arap, R. Pasqualini, E. Ruoslahti, Science 279 (1998) 377.
[131] Z. Varpness, J.W. Peters, M. Young, T. Douglas, Nano Lett. 5 (2005) 2306.
[132] R. Cammack, Nature 397 (1999) 214.